

# Inhibiting Platelet-derived Growth Factor $\beta$ Reduces Ewing's Sarcoma Growth and Metastasis in a Novel Orthotopic Human Xenograft Model

YONG XIN WANG<sup>1</sup>, DEENDAYAL MANDAL<sup>5</sup>, SUIZHAU WANG<sup>2</sup>, DENNIS HUGHES<sup>1</sup>,  
RAPHAEL E. POLLOCK<sup>3</sup>, DINA LEV<sup>4</sup>, EUGENIE KLEINERMAN<sup>1</sup> and ANDREA HAYES-JORDAN<sup>3</sup>

*Departments of <sup>1</sup>Pediatrics, <sup>2</sup>Genetics, <sup>3</sup>Surgical Oncology, and <sup>4</sup>Cancer Biology,  
The University of Texas M.D. Anderson Cancer Center, Houston, TX 77030;*

*<sup>5</sup>Biomedical and Pharmaceutical Sciences, University of Rhode Island, Kingston, RI 02881, U.S.A.*

**Abstract.** *Background: Despite aggressive therapy, Ewing's sarcoma (ES) patients have a poor five-year overall survival of only 20-40%. Pulmonary metastasis is the most common form of demise in these patients. The pathogenesis of pulmonary metastasis is poorly understood and few orthotopic models exist that allow study of spontaneous pulmonary metastasis in ES. Materials and Methods: We have developed a novel orthotopic xenograft model in which spontaneous pulmonary metastases develop. While the underlying biology of ES is incompletely understood, in addition to the EWS-FLI-1 mutation, it is known that platelet-derived growth factor receptor  $\beta$  (PDGFR- $\beta$ ) is highly expressed in ES. Hypothesizing that PDGFR- $\beta$  expression is indicative of a specific role for this receptor protein in ES progression, the effect of PDGFR- $\beta$  inhibition on ES growth and metastasis was assessed in this novel orthotopic ES model. Results: Silencing PDGFR- $\beta$  reduced spontaneous growth and metastasis in ES. Conclusion: Preclinical therapeutically relevant findings such as these may ultimately lead to new treatment initiatives in ES.*

Ewing's sarcoma (ES) is a primitive neuroectodermal tumor that most often affects children and young adults between 5 and 30 years of age; it is the second most common bone tumor in children (1). Despite multidisciplinary care algorithms for ES that include surgical resection, chemotherapy and radiotherapy,

survival for afflicted patients remains dismal at 20-40% at five years, and has not improved for patients with metastasis since the mid-1970s (1-3). This lack of progress in ES treatment is particularly ominous for patients with metastatic disease in which the disease is rapidly lethal in 80-90%, with the remainder usually succumbing over a slightly longer time course.

Progress in developing new treatments for metastatic ES has been limited by a fundamental lack of murine models that accurately mimic human primary and metastatic disease. Antecedent murine ES xenograft models have generally utilized heterotopic subcutaneous human ES cell suspension injection (4, 5), other ES models have used experimental intravenous injection of human ES tumor cells that home to the lungs (6). Such models are flawed by either lack of orthotopic ES inoculation sites, or by the use of intravenous ES cell injection to experimentally generate pulmonary metastases which obviates the selection pressures exerted by the initial steps in the metastatic cascade, *i.e.* interaction with the tumor-modulating microenvironment, tumor cell extravasation processes across the basement membrane, and subsequent ES invasion into the systemic vasculature.

Lacking truly relevant *in vivo* models of human ES, it has not been possible to target the unique aspects of ES needed to develop new pre-clinical therapeutic strategies. In light of these issues, we created a unique ES model utilizing orthotopic cell injection into the bone resulting in subsequent spontaneous pulmonary metastasis, thereby more closely approximating the natural clinical history of human ES. Since platelet-derived growth factor receptor  $\beta$  (PDGFR- $\beta$ ) is highly expressed in ES and regulates cell motility and growth (7), (shRNA) was used to silence PDGFR- $\beta$  using this model and the inhibition of both local tumor growth and spontaneous pulmonary metastasis were increased.

*Correspondence to:* Andrea Hayes-Jordan, MD, Department of Surgical Oncology, The University of Texas M. D. Anderson Cancer Center, 1515 Holcombe Blvd, Unit 444, Houston TX 77030, U.S.A. Tel: +17137944258, Fax: +17137451921, e-mail: ahjordan@mdanderson.org

*Key Words:* PDGFR- $\beta$ , Ewing's sarcoma, orthotopic.

## Materials and Methods

**Orthotopic chest wall model.** Approval was obtained from our Institution Animal Care and Use Committee. Approximately 8-week-old, 25 g, female athymic, nude (nu/nu) mice were obtained from the National Cancer Institute. A total of 500,000 cells (TC71 or TC71pds) were suspended in 20  $\mu$ L of (PBS). After induction of anesthesia an incision was made in the posterior-lateral chest wall, after which cells were injected into the nude mouse periosteum of the lower rib using a 27 gauge needle at  $\times 1.5$  magnification; the wound was then closed with sutures. All mice were monitored for full recovery after anesthesia. Mice were examined daily and tumors measured three times/week using calipers. Mice which developed chest wall tumors were sacrificed after tumors reached a maximum of 1.5 cm in size. Mice with no external chest wall tumors were sacrificed when they became lethargic or tachypneic. There were 9 mice in each group; experiments were repeated twice and results are reported as a total of both experiments. All animals underwent complete necropsy. For subsequent quantification of tumor volume, bioluminescent imaging was used (see below).

**shRNA PDGFR- $\beta$  preparation.** shRNA expression vector pSilencer2.1-U6 hygro was purchased from Ambion (Austin, TX, USA). Plasmids that express shRNA and target human PDGFR- $\beta$  were constructed according to the manufacturers instructions. Briefly, four pairs of cDNA oligonucleotides targeting human PDGFR- $\beta$  mRNA at four different locations were synthesized by Integrated DNA Technologies (Coralville, IA, USA). Each pair of oligonucleotides was annealed at 90°C for 3 minutes, cooled to 37°C, and incubated for 1 hour. The annealed double-stranded DNA oligonucleotides were ligated between the *Bam*HI and *Hind*III sites on the pSilencer2.1-U6 hygro vector. The control vector (non-targeting shRNA) was constructed by inserting a sequence that expresses limited homology to sequences in the human and mouse genomes. The targeted PDGFR- $\beta$  sequences were: I) AACTATTCATCTTTCTCACGG; II) AATGAGGTGGTCAACTTCGAG; III) AAGGTGATTGAGTCTGTGAGC; IV) AATGAAGTCAACACCTCCTCA and pdsh control: CTACCGTTGTTATAGGTG TCTCTTGAACACCTATAACAACGGTAGT. All inserted sequences were verified by DNA sequencing. Transfections were carried out with Superfect (Qiagen, Valencia, CA, USA) as directed by the manufacturer and selected in medium containing hygromycin B (Invitrogen LifeTechnologies, Carlsbad, CA, USA) at 400  $\mu$ g/ml for TC71 cells. Stable transfected cell clones were tested for PDGFR- $\beta$  expression by RT-PCR and Western blot. PDGFR- $\beta$  shRNA used in these experiments were derived from a single clone named TC-71 pdsh. TC-71 cells which were transfected with a nonsense sequence were named TC-71pd cells. This cell line was used as a control. Figure 6 demonstrates 'silencing' of PDGFR- $\beta$  by RT-PCR.

**Cell culture and transfection.** TC71 human Ewing's sarcoma cells were cultured as described elsewhere (8, 9). To create luciferase-labeled tumor cells, the full-length firefly luciferase gene was spliced into the MigR1 expression vector and viral particles generated as described elsewhere (10). TC71 cells were transduced on two consecutive days with infectious supernatant, then incubated for 48 hours to allow for expression of incorporated retrovirus. Expression of (EGFP), present as the second cistron in

the expression cassette and translated under the direction of an internal ribosomal entry sequence, was confirmed *via* direct fluorescent microscopy. Transduced cells were purified *via* flow cytometry to select EGFP-expressing cells and luciferase expression was confirmed by visible light emission upon addition of luciferin.

**Bioluminescent imaging.** After the injection of cells, the mice were imaged at different time points using an *in vivo* IVIS 100 bioluminescence/optical imaging system (Xenogen, Alameda, CA, USA). D-Luciferin (Xenogen) dissolved in (PBS) was injected *i.p.* at a dose of 150 mg/kg 10 minutes before measuring the light emission. General anesthesia was induced with 5% isoflurane and continued during the procedure. After acquiring photographic images of each mouse, luminescent images were acquired with various (1-60 seconds) exposure times. The resulting grayscale photographic and pseudocolor luminescent images were automatically superimposed by the IVIS Living Image (Xenogen) software to facilitate matching the observed luciferase signal with its location on the mouse. Regions of interest (ROI) were manually drawn around the bodies of the mice to assess signal intensity emitted. Luminescent signal was expressed as photons per second emitted within the given ROI. Tumor bioluminescence in mice linearly correlated with the tumor volume (11).

**Reverse transcriptase polymerase chain reaction (RT-PCR).** To study mRNA expression for PDGFR- $\beta$  *in vitro* in cell lines and *in vivo*, total RNA extraction and semi-quantitative reverse transcription-PCR were carried out on tissues and cell lines. PCR reactions were optimized for the number of cycles to ensure product intensity within the linear phase of amplification. Quantification of the signals was performed by densitometric analysis (Kodak Digital Science) after normalizing individual bands to the respective 18 S bands.

**Western immunoblotting (WB).** WB was performed briefly as follows: 50  $\mu$ g of proteins extracted from cultured cells were separated by SDS-PAGE and transferred onto nitrocellulose membranes (Millipore Co, Bedford, MA); membranes were blocked and blotted with relevant antibodies. Horseradish peroxidase-conjugated secondary antibodies were detected by ECL chemiluminescence (Amersham Biosciences, Plc., UK). IRdye680- and IRdye800-conjugated secondary antibodies (Molecular Probes, Eugene, OR, USA) were detected using Odyssey Imaging (LICOR Biosciences, Lincoln, NE, USA). Figure 6 demonstrates 'silencing' of PDGFR- $\beta$  by Western blotting

## Results

**A novel orthotopic xenograft model of ES.** Orthotopic models more closely resemble human disease compared to heterotopic systems in that the former permit study of tumor: microenvironment interactions that potentially reflect such processes as known to occur in patients. Since ES primarily originates in long and flat bones, we sought to more closely replicate the human disease by injecting human TC71 ES cells directly into the relatively soft rib bone of the nude mouse which can be directly visualized after division of the skin and separation of muscles overlying the posterior lateral chest wall. Three distinctly separate patterns of

disease resulted from this modeling approach. Approximately 60% of mice developed tumors only at the chest wall site of orthotopic ES inoculation (Figure 1). Most tumors grew to 1 cm in 21 to 28 days after inoculation. As in humans, these tumors grow in an extrathoracic manner, expanding from the rib to the skin (Figure 1a) while infiltrating between ribs to access the intrathoracic cavity (Figure 1c, d, and e).

Approximately 30% of the mice developed bilateral pulmonary metastases without evidence of significant chest wall involvement (Figure 1b). Mice lacking demonstrable chest wall tumor by 14 days after injection were found to have developed pulmonary metastatic disease upon sacrifice at different time points thereafter. Mice were sacrificed weekly or until systemic signs of respiratory compromise were evident. These mice uniformly had bilateral pulmonary metastases which were parenchymal and did not represent 'spill' from the injection site. Tumors were nodular and present in all lobes of both lungs.

Approximately 10% of mice demonstrated both injection site chest wall tumors and pulmonary metastases. Chest wall tumors ranged in size from 5-10 mm at day 13-17 after inoculation, before pulmonary metastases were evident one to 2 weeks later. Again over time, pulmonary metastases were bilateral in all animals.

To establish the temporal kinetics of this metastatic process, mice were then injected with luciferase-labeled TC71 ES cells (Figure 2). In figure 2a, a large tumor can be seen on the chest wall at 20 days after injection. The animal in Figure 1b was injected on the right chest wall and small pulmonary metastases are visible on the opposite lung; in contrast, Figure 2c and 2d show simultaneous growth of chest wall tumor and lung metastases. Unilateral pulmonary metastases were detected at early time points after ES inoculation into the rib, whereas bilateral spontaneous pulmonary metastases were typically observed at later times (Figure 2c, d).

TC71 lung metastases were extracted, expanded in culture and then re-injected into the rib in the orthotopic locus. This daughter cell line of TC71 is named TC-W. In repeat experiments, 5 out of 10 and 7 out of 12 TC-W injected mice developed pulmonary metastases, whereas the remainder (9/22) developed local chest wall tumors. The incidence of metastasis from the TC-W tumor cells was 54% compared to 30% from the TC71 parental tumor cells ( $p=0.01$ ). Weights of TC-W tumors are shown in Figure 3.

*Effect of PDGFR- $\beta$  inhibition on tumor formation and metastasis in vivo in the ES orthotopic xenograft model.* PDGFR- $\beta$  is highly expressed in ES cells and human ES tumors (7). Using shRNA, the PDGFR- $\beta$  gene in human TC71 cells was silenced, resulting in significant PDGFR- $\beta$  RNA and protein knock down in one clone, which was named TC71pdsh and selected for use in subsequent studies. We measured the effect of PDGFR- $\beta$  inhibition on the growth and

metastasis of ES in two ways. Using this orthotopic xenograft model we first measured the rate of tumor growth and incidence of spontaneous metastasis by direct measurement of the chest wall tumors and weights of the extracted lungs as compared to controls. We found a significant lag in growth and lower size of primary chest wall ES tumors ( $p<0.01$ ), and significant decrease in pulmonary metastases ( $p<0.05$ ) in the PDGFR- $\beta$ -silenced tumors (Figure 4a, b).

Luciferase-transfected TC71 or TC71pdsh cells were injected into the rib as described above and tumor sizes were compared by bioluminescent imaging. We measured significantly smaller tumors in the TC71pdsh-injected mice ( $p=0.0175$ ) versus TC71 derived tumors (Figure 5a-d). Similarly, pulmonary metastatic growth was found to be significantly lower in the TC71pdsh-injected mice ( $p=0.02$ ) versus that from TC71 derived tumors (Figure 5e-h).

## Discussion

In this novel model, it was possible to observe spontaneous pulmonary metastasis after orthotopic ES implantation. Primary tumor growth and pulmonary metastasis could be inhibited by silencing PDGFR- $\beta$ . This model differs from other ES models using *e.g.* experimental tail vein injection to generate pulmonary metastasis or heterotopic primary tumor site implantations (12-14). While tail vein injection models may be used to effectively address the consequences of pulmonary metastasis, determining the drivers of spontaneous pulmonary metastasis usually mandates models that more directly mimic this process. This model, in contrast to heterotopic models, also allows study of ES primary tumors in their natural microenvironment *i.e.* the bone, where other early steps in the metastatic cascade may potentially be more realistically assessed.

When using a NOD/SCID mouse model, Vormoor *et al.* found 40-50% transplant efficiency of ES using subcutaneous (*s.c.*) or intravenous (*i.v.*) injection (6). In another study by Scotlandi *et al.*, three different ES cell lines were injected *s.c.* or *i.v.* into athymic mice; they found 0-40% efficiency in primary tumor formation, lung and bone metastasis (13). However, these models do not accurately mimic what occurs in the clinical setting. In ES, tumors arise in the bone and, over time if not effectively treated, spread to lungs or other bone sites. Analogous to the clinical reality, in our model, the tumor begins in the bone; as with ES patients, some mice have tumor only at the primary site, whereas others demonstrate spontaneous spread from the primary site of injection to other sites such as the lungs.

In the model by Vormoor *et al.* and murine tail vein injection models, tumor formation efficiency ranges from 0 to 50% (13), whereas in our model all mice develop primary and/or pulmonary metastatic disease. A possible explanation why some animals develop pulmonary metastasis whereas others only develop chest wall tumors may involve clonal

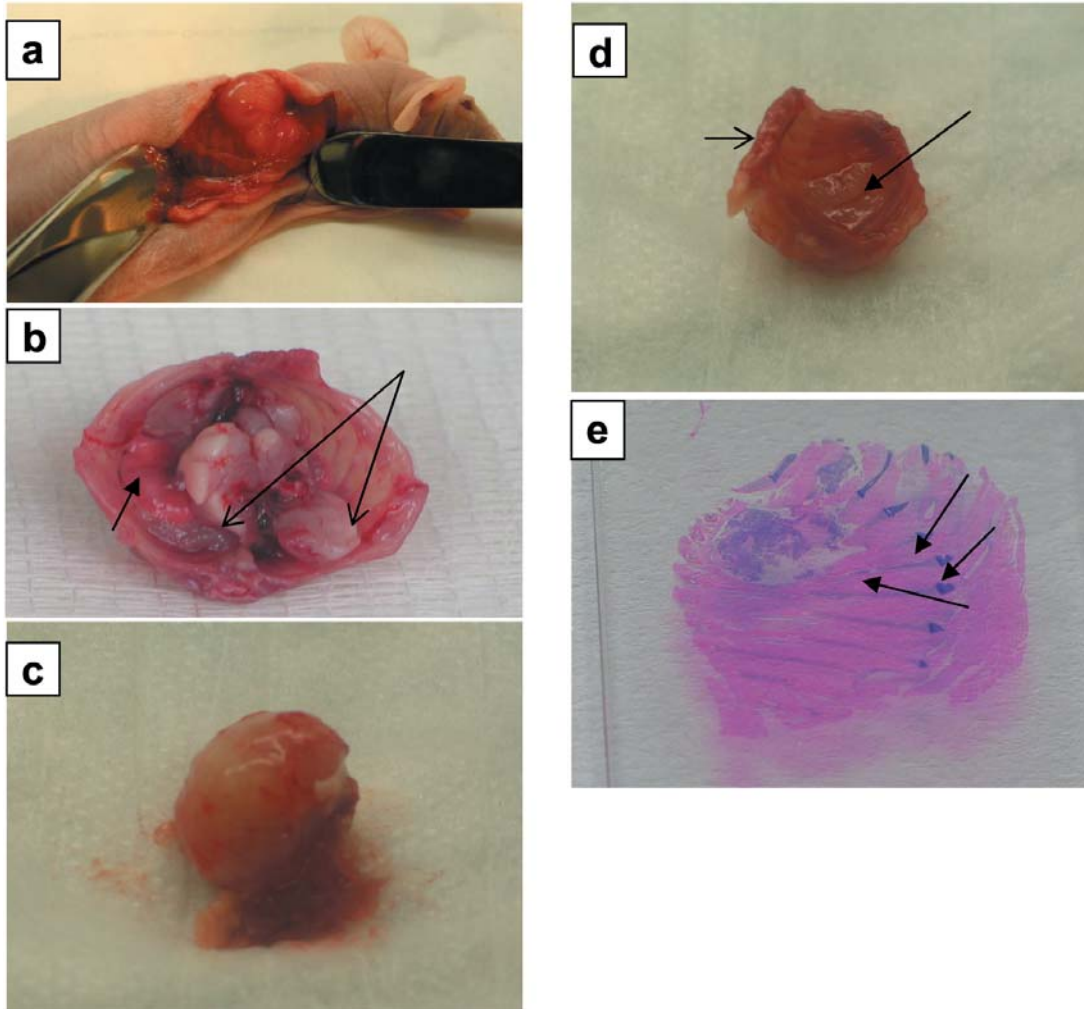


Figure 1. *a*, Orthotopic chest wall tumor; *b*, bilateral pulmonary metastases (line arrows) in mouse thoracic cavity, solid arrow denotes remaining normal lung; *c*, dorsal surface of chest wall tumor ex vivo; *d*, parietal pleural surface of chest wall Ewing's sarcoma: solid arrow denotes tumor pushing between the ribs, line arrow denotes spine; *e*, H&E stain of orthotopic tumor (line arrow) between ribs (solid arrow).

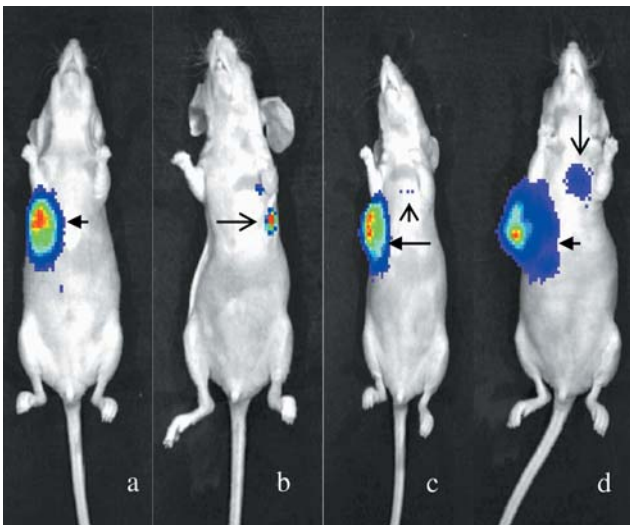


Figure 2. *a*, Solid arrow indicates chest wall tumor 20 days after orthotopic injection of TC71 Ewing's sarcoma cells. No pulmonary metastases were seen in 65% of mice. *b*, Line arrow indicates early pulmonary metastasis at 18 days after injection of TC71 Ewing's sarcoma cells. No chest wall tumor was seen in 25-30% of mice. Chest wall tumor and pulmonary metastasis at 16 (*c*) and 22 (*d*) days post injection (~10% of mice had this phenotype).

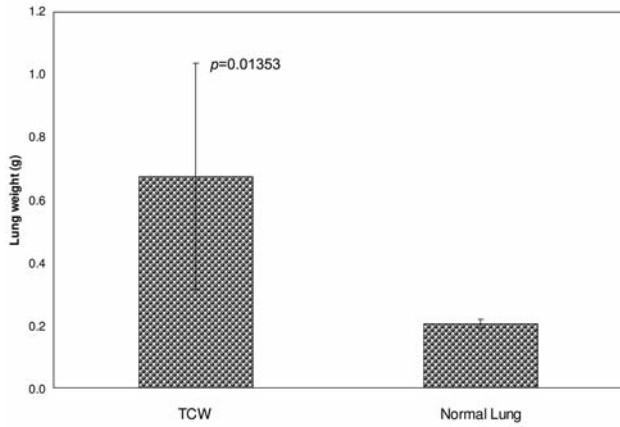


Figure 3. Lung weights of TC-W (expanded from TC71 lung metastasis) lung metastases compared to normal lung.

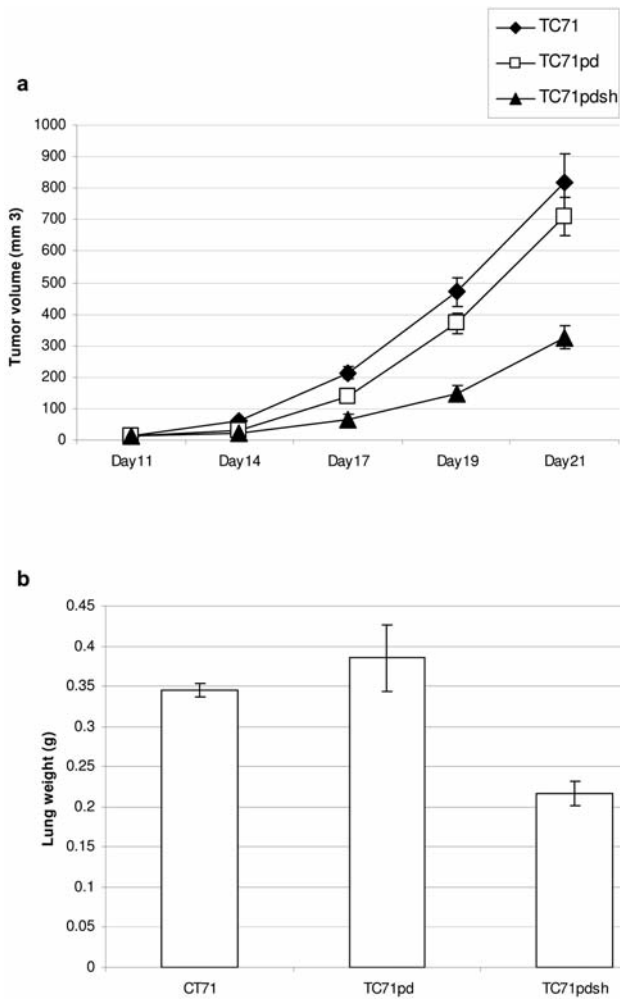


Figure 4. a, Size of orthotopic chest wall tumors from mice injected with parental cell (TC71, scrambled vector (TC71pd) and PDGFR- $\beta$  silenced (TC71pdsh) cells;  $p < 0.01$ . b, Weights of lungs per mouse in TC71 compared to TC71pd and TC-71pdsh inoculated mice;  $p < 0.05$ .

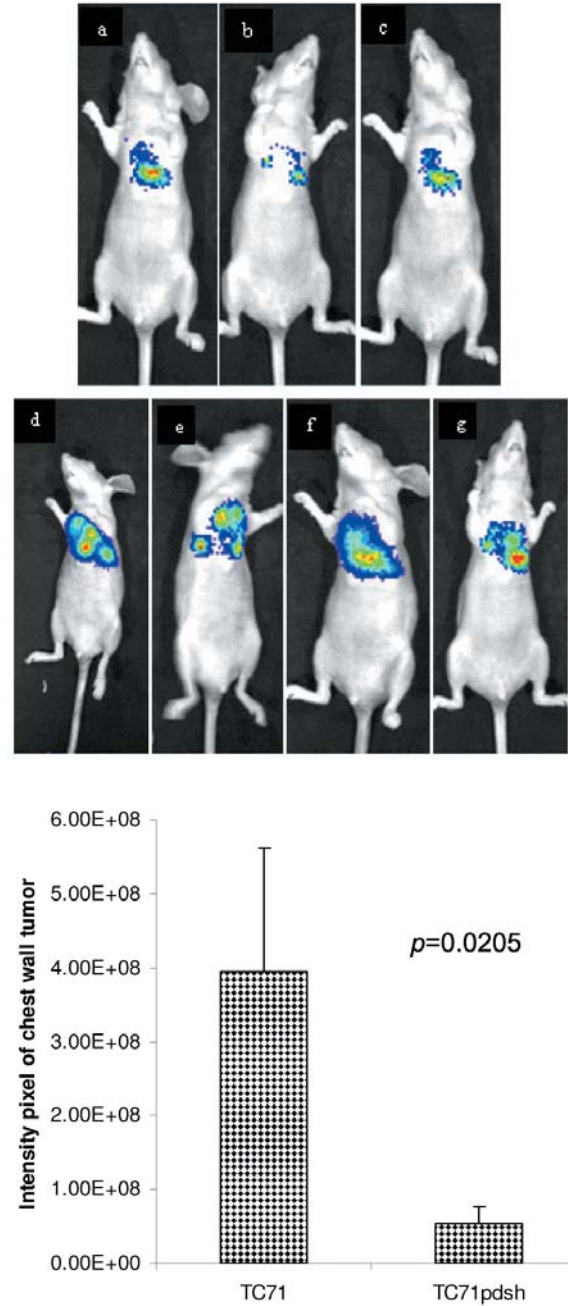


Figure 5. (a-c): Growth comparison of pulmonary metastases 21 days after injection of human Ewing's sarcoma tumor cells into the rib of nude mice. Primary tumor size was statistically significantly smaller in PDGFR- $\beta$ -silenced ES tumors, TC71pdsh (d-g), compared to control tumors, TC71.

expansion of ES cells having greater metastatic potential: when cells from the orthotopic xenograft pulmonary metastasis were re-cultured and subsequently re-injected, a larger percentage of mice developed pulmonary metastasis.

ES is one of the few sarcomas expressing high levels of PDGFR- $\beta$ , which has been shown to mediate tumor cell

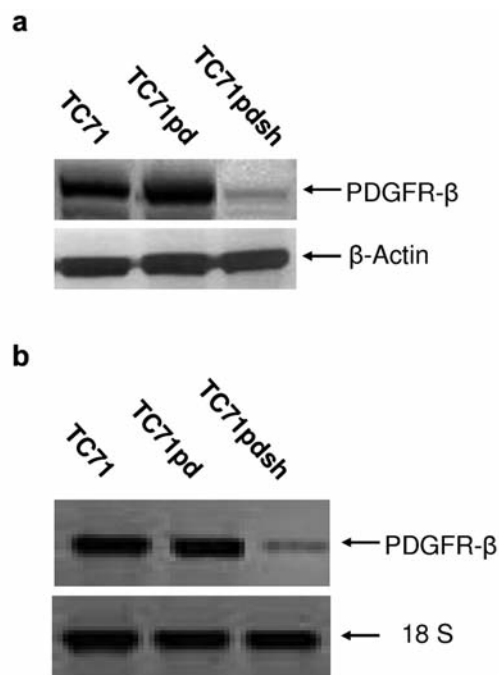


Figure 6. a) Western blot of the shRNA PDGFR-B. b) RT-PCR of the shRNA for PDGFR-B.

motility and growth in this disease (7). Others have demonstrated that administration of PDGFR-β inhibitors in murine models of various tumor types results in lower tumor growth and angiogenesis (7, 15, 16). In renal cell carcinoma in which increased PDGFR-β expression is also observed, in a preclinical model, others have shown that PDGFR-β inhibition *via* administration of siRNA slows tumor growth (17).

Imatinib mesylate (Gleevec™), a tyrosine kinase inhibitor that targets PDGFR-β, has been used in a phase II study for children with recurrent ES. In this trial, imatinib mesylate was used as a single agent, and only 1 out of 24 patients had a response (18). In contrast, when imatinib mesylate was used *in vitro* in combination with an insulin growth factor receptor (IGFR) inhibitor, 70% cell death was observed in ES cell lines (19), suggesting the possibility of synergistic use in the clinical setting. In ongoing studies, an IGFR inhibitor as a single agent has been used for ES patients, with promising preliminary results (19). Preclinical testing of these and other therapeutic possibilities in a spontaneous metastasis model of ES such as the one described here may offer fresh insight into new and effective treatments for this devastating disease. Given that ES patients who develop pulmonary metastasis have a 10% rate of overall survival, the urgency underlying the need for new treatment approaches is apparent and cannot be understated.

## Acknowledgements

This work was supported by the Robert Wood Johnson Foundation Harold Amos Award.

## References

- Gurney JG, Severson RK, Davis S and Robison LL: Incidence of cancer in children in the United States. Sex-, race-, and 1-year age-specific rates by histologic type. *Cancer* 75: 2186-2195, 1995.
- Horowitz ME, Kinsella TJ, Wexler LH, Belasco J, Triche T, Tsokos M, Steinberg SM, McClure L, Longo DL, Steis RG *et al*: Total-body irradiation and autologous bone marrow transplant in the treatment of high-risk Ewing's sarcoma and rhabdomyosarcoma. *J Clin Oncol* 11: 1911-1918, 1993.
- Wexler LH, DeLaney TF, Tsokos M, Avila N, Steinberg SM, Weaver-McClure L, Jacobson J, Jarosinski P, Hijazi YM, Balis FM and Horowitz ME: Ifosfamide and etoposide plus vincristine, doxorubicin, and cyclophosphamide for newly diagnosed Ewing's sarcoma family of tumors. *Cancer* 78: 901-911, 1996.
- Bolontrade MF, Zhou RR and Kleinerman ES: Vasculogenesis plays a role in the growth of Ewing's sarcoma *in vivo*. *Clin Cancer Res* 8: 3622-3627, 2002.
- Guan H, Zhou Z, Wang H, Jia SF, Liu W and Kleinerman ES: A small interfering RNA targeting vascular endothelial growth factor inhibits Ewing's sarcoma growth in a xenograft mouse model. *Clin Cancer Res* 11: 2662-2669, 2005.
- Vormoor J, Baersch G, Decker S, Hotfilder M, Schafer KL, Pelken L, Rube C, Van Valen F, Jurgens H and Dockhorn-Dworniczak B: Establishment of an *in vivo* model for pediatric Ewing tumors by transplantation into NOD/scid mice. *Pediatr Res* 49: 332-341, 2001.
- Uren A, Merchant MS, Sun CJ, Vitolo MI, Sun Y, Tsokos M, Illei PB, Ladanyi M, Passaniti A, Mackall C and Toretsky JA: Beta-platelet-derived growth factor receptor mediates motility and growth of Ewing's sarcoma cells. *Oncogene* 22: 2334-2342, 2003.
- Jia SF, Zhou RR and Kleinerman ES: Nude mouse lung metastases models of osteosarcoma and Ewing's sarcoma for evaluating new therapeutic strategies. *Methods Mol Med* 74: 495-505, 2003.
- Lee TH, Bolontrade MF, Worth LL, Guan H, Ellis LM and Kleinerman ES: Production of VEGF165 by Ewing's sarcoma cells induces vasculogenesis and the incorporation of CD34+ stem cells into the expanding tumor vasculature. *Int J Cancer* 119: 839-846, 2006.
- Tatsuguchi A, Matsui K, Shinji Y, Gudis K, Tsukui T, Kishida T, Fukuda Y, Sugisaki Y, Tokunaga A, Tajiri T and Sakamoto C: Cyclooxygenase-2 expression correlates with angiogenesis and apoptosis in gastric cancer tissue. *Hum Pathol* 35: 488-495, 2004.
- Zhang P, Yang Y, Zweidler-McKay PA and Hughes DP: Critical role of notch signaling in osteosarcoma invasion and metastasis. *Clin Cancer Res* 14: 2962-2969, 2008.
- Hu-Lieskovan S, Heidel JD, Bartlett DW, Davis ME and Triche TJ: Sequence-specific knockdown of EWS-FLI1 by targeted, nonviral delivery of small interfering RNA inhibits tumor growth in a murine model of metastatic Ewing's sarcoma. *Cancer Res* 65: 8984-8992, 2005.

- 13 Scotlandi K, Benini S, Manara MC, Serra M, Nanni P, Lollini PL, Nicoletti G, Landuzzi L, Chano T, Picci P and Baldini N: Murine model for skeletal metastases of Ewing's sarcoma. *J Orthop Res* 18: 959-966, 2000.
- 14 Castillero-Trejo Y, Eliazar S, Xiang L, Richardson JA and Ilaria RL Jr: Expression of the EWS/FLI-1 oncogene in murine primary bone-derived cells Results in EWS/FLI-1-dependent, ewing sarcoma-like tumors. *Cancer Res* 65: 8698-8705, 2005.
- 15 Armulik A, Abramsson A and Betsholtz C: Endothelial/pericyte interactions. *Circ Res* 97: 512-523, 2005.
- 16 Hellstrom M, Gerhardt H, Kalen M, Li X, Eriksson U, Wolburg H and Betsholtz C: Lack of pericytes leads to endothelial hyperplasia and abnormal vascular morphogenesis. *J Cell Biol* 153: 543-553, 2001.
- 17 Xu L, Tong R, Cochran DM and Jain RK: Blocking platelet-derived growth factor-D/platelet-derived growth factor receptor beta signaling inhibits human renal cell carcinoma progression in an orthotopic mouse model. *Cancer Res* 65: 5711-5719, 2005.
- 18 Bond M, Bernstein ML, Pappo A, Schultz KR, Krailo M, Blaney SM and Adamson PC: A phase II study of imatinib mesylate in children with refractory or relapsed solid tumors: a Children's Oncology Group study. *Pediatr Blood Cancer* 50: 254-258, 2008.
- 19 Martins AS, Mackintosh C, Martin DH, Campos M, Hernandez T, Ordonez JL and de Alava E: Insulin-like growth factor I receptor pathway inhibition by ADW742, alone or in combination with imatinib, doxorubicin, or vincristine, is a novel therapeutic approach in Ewing tumor. *Clin Cancer Res* 12: 3532-3540, 2006.

*Received May 12, 2009*

*Revised August 21, 2009*

*Accepted September 21, 2009*